Time-domain terahertz spectrometer for angular reflection measurements

2015 J. Phys.: Conf. Ser. 605 012026

(http://iopscience.iop.org/1742-6596/605/1/012026)

Journal of Physics: Conference Series **605** (2015) 012026 doi:10.1088/1742-6596/605/1/012026

Time-domain terahertz spectrometer for angular reflection measurements

José Antonio Nóvoa[1], Ismael Ordoñez[1], Carmen Rial[2], Jorge Martín[1], Álvaro Gil[2] and José Ramón Salgueiro[1]

[1]Departamento de Física Aplicada, Universidade de Vigo, As Lagoas, s/n, 32004 Ourense, Spain

[2]Instituto de Cerámica de Galicia, Universidade de Santiago de Compostela, Campus Sur, 15782 Santiago de Compostela, Spain

E-mail: joseantonionolo@gmail.com

Abstract. We describe a terahertz time-domain spectrometer developed to perform measurements by reflection under a wide range of angles. The different parts of the device are described as well as the process of frequency-scale calibration and signal linearity evaluation. Also the main parameters that characterize the system and account their performance are measured. Finally an example of application to the measurement of the bandgap of a photonic crystal designed for the terahertz band is presented.

1. Introduction

The terahertz (THz) electromagnetic band, in the range between 0.1 and 10 THz which corresponds to wavelengths between 3 mm and 30 μm respectively, has recently been the object of an intense research activity because of the finding of novel and interesting applications [1–5]. It had been to great extent neglected up to know because of the strong absorption of the atmosphere at these frequencies what made them useless for telecommunications and also because the available sources were scarce and inefficient. The traditional interest on this radiation came on one hand from radioastronomers who wanted to work with increasingly shorter wavelengths, and from spectroscopists who wanted to work at increasingly longer wavelengths in the infrared.

The recent development of efficient sources of such radiation has made possible to apply THz technology to a number of fields, remarkably tomography and spectroscopy. In fact, THz techniques are useful for non-destructive diagnostic as for instance early detection of internal caries or tumoral cells [6–8]. This is due to the fact that water strongly absorbs at this band and so it results easy to distinguish between tissues with slightly different water content. On the other hand this radiation is very useful for the structural analysis of materials and complex molecules [9]. Many molecules that are key components of drugs or explosives have a characteristic spectrum at these frequencies and so the detection of such substances becomes possible, leading to the use of this technology for safety applications [10–12]. Besides, it allows to distinguish among different types of materials, measure density of dopants and detect and measure pollution gases [13, 14].

One of the cheapest ways to generate THz radiation is by means of the photoconductive effect[5]. It requires from an ultrashort pulsed laser source that is used to irradiate an antenna

made of two close conductors (forming a gap) attached to a semiconductor material. A bias voltage is applied to the conductors in order to generate an electric field. The laser pulse promotes charge carriers from the valence band to the conduction band which are then accelerated by the field producing the THz radiation. Using a pulsed laser of a particular repetition rate results in a train of THz pulses known as T-rays. The detection of the THz radiation can be carried out using the same effect. In this case the incoming THz pulse, impinging on the antenna synchronously with the laser pulse, moves the promoted carriers generating a small current that can be detected, amplified and measured. A controlled time delay in this laser pulse allows to scan the THz pulse and directly measure the electric field as a function of time.

The production and detection mechanisms described above are the basis of the successful time domain spectroscopy technique (THz-TDS) [3, 5], which is now one of the most versatile and cheapest for many applications, particularly for material analysis. A number of spectrometers were already described in the literature and the THz-TDS is at the moment a recent but quite well established technique [5, 15–17]. Most of the described spectrometers, however, are based on measuring radiation transmitted by the sample under analysis. THz-TDS technique based on measurements by reflection is quite scarcely used [18–20] because it results technically more complicated since the emitter and/or receiver must be mobile devices and that makes alignment more difficult. Reflection measurements under different angles are, however, interesting for many applications as they provide information that transmission not always can provide, for instance when the material under study is deposited on a substrate surface or for high absorbent bulk materials. This makes a reflection spectrometer a very useful tool.

In this work we describe our developed spectrometer for making reflection measurements for a broad range of angles. In the following section, a description of the set up is carried out. In section 3 we present the results of the calibration process as well as the parameter evaluation that accounts for the device performance. Finally, section 4 is devoted to show an example of application to the measurement of the bandgap of a photonic crystal.

2. Description of the spectrometer

A scheme of the developed set up is shown in figure 1. In order to make possible the recording of measurements under different angles, the receptor is mounted on a bench attached to a rotating stage. On the other hand the sample holder is also mounted on another rotating stage to properly orientate the sample respect to the impinging THz beam. A beam from a Ti-Za pulsed laser (wavelength $\lambda = 810\,\mathrm{nm}$, pulse duration 75 fs, and repetition rate 80 MHz) is divided in two beams to feed both emitter and receiver photoconductive antennas. In order to assure the mobility of the receiver, the corresponding beam is coupled to a 1 m long optical fiber. The output of the fiber is coupled to a beam collimator installed on the receiver head, properly aligned to feed the lens that focuses it on the antenna gap. On the other hand, the other beam is also directed to the emitter using an identical piece of fiber in order to compensate for optical path and pulse widening due to dispersion. In such a way two similar synchronized pulses are used for both emitter and receiver. In order to scan the THz pulse a delay line, consisting in a motorized stage that displaces a mirror, is installed in the path of the beam directed to the receiver. In such a way, it is possible to change the time delay between both pulses directed to emitter and receiver. Programming the scanning stage to run at a fixed velocity a set of measurements of the THz-electric field are taken for different delay times. A polarizing beam splitter and a combination of a half and a quarter wave plates are used to properly separate the two fractions of the laser beam used for the emitter and receiver.

The output of the receiving antenna is a current in the range of the tenths of nA which is transformed into a voltage using a low-noise transimpedance preamplifier with a gain about $10^5\,\mathrm{V/A}$ and then further enhanced using a lock-in amplifier. The output of the lock-in amplifier

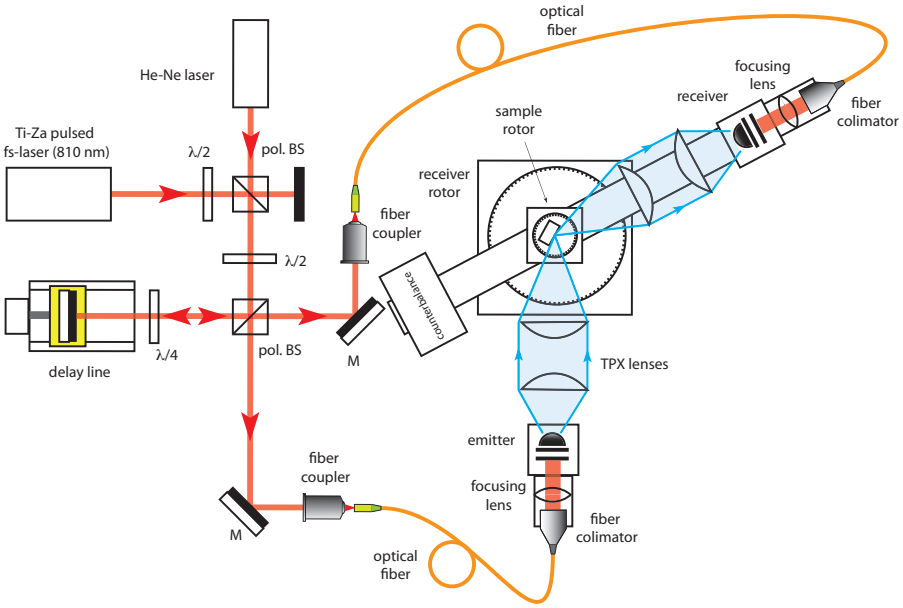

Figure 1: Sketch of the spectrometer set up.

is read by a data acquisition device on the same computer controlling the delay line. In this way, measurements are automatically taken. In combination with the lock-in amplifier, an electronic chopper is used to drive the emitter bias voltage as an square signal of frequency about 15 kHz and amplitude of 30 V (the required by the antennas used). To maximize the efficiency, instead of periodically interrupting the bias voltage the polarity is inverted at every half period, so that emission of THz radiation is never interrupted and a periodic phase change is introduced in the signal, enough to make the lock-in amplifier to work. This solution also introduces periodic phase changes in the THz radiation but they have no effect as those are produced at a rate between four and five magnitude orders slower than the pulse repetition rate.

The set up also includes an He-Ne laser whose beam is superposed to the Ti-Za laser in order to perform the system alignment more comfortably and safely. Besides, a half wave plate and a polarizing beam splitter are used at the beam input to adjust power which should not rise over 10 mW to avoid damage of the antennas.

3. Spectrometer evaluation

In order to tune the spectrometer and assess its performance a calibration process as well as an evaluation of the main characteristic parameters is necessary. To be precise, the frequency scale has to be calibrated to assure accurate measurements and also the linearity of the output checked. Considering that our assembly is a reflection spectrometer, both frequency and linearity calibrations will be defined for zero angle. The process is completed with the measurement of the signal to noise ratio, dynamic range, spectral resolution and THz electric field of the generated THz radiation.

3.1. Frequency calibration

As we have described before, a THz-TDS spectrometer works in the time domain and the use of an FFT algorithm is needed to get the frequency spectrum. Therefore, the frequency scale must be ensured externally. Many methods and techniques have been developed but most of them are based in a contrast pattern, consisting in the use of a material with a known THz spectrum which is compared to the spectrum obtained from the set up. Two common possibilities are the

use of the absorption spectrum from a gas or the frequency pattern of an etalon [21]. The first one involves the use of a external database and is more expensive than the etalon. Thus, we chose an etalon-based calibration. Our etalon is a plane parallel plate of pure silicon with both faces optically polished that forms a Fabry-Perot interferometer and generates a peak pattern when it is introduced in the path of the THz beam.

If n is the refractive index of the etalon material, l its thickness and N an integer describing the order of the peak, corresponding to the number of wavelengths in the etalon, the frequencies for the peaks and valleys are given by the expressions

$$f_N = \frac{c}{2nl}N; \qquad \text{peaks} \tag{1}$$

$$f_{N+\frac{1}{2}} = \frac{c}{2nl}\left(N+\frac{1}{2}\right); \qquad \text{valleys.} \tag{2}$$

According to the Fabry-Perot interferometer theory, the model for reflectance R and transmittance T to compare with the measured spectrum is mathematically described by

$$R = \left(\frac{n-1}{n+1}\right)^2; \quad \delta = 4\pi nl\frac{f}{c}, \tag{3}$$

$$T = \left(1+F\sin^2\frac{\delta}{2}\right)^{-1}; \quad F = \frac{4R}{(1-R)^2}, \tag{4}$$

$$\tag{5}$$

where δ is the phase difference induced by the etalon and F the finesse coefficient. Using the characteristics of the etalon, we will get a theoretical model for the frequency transmitted through the etalon. With this model we can estimate the correlation between the theory and the spectrum obtained from THz-TDS. We used an etalon with a thickness of $l = 0.5\,\text{mm}$ and refractive index $n = 3.42$. In figure 2 it is shown the transmittance (angle zero) obtained from this theoretical model (dashed line) superposed to the measured signal (continuous line). There is a pretty close match between model and experimental results, and the measured peaks can be identified with those of the model to calibrate the frequency scale.

3.2. Linearity calibration

Ensuring a linear response of the spectrometer is very important because the frequency spectrum of a substance should be independent of the sample thickness. So, if the spectrometer has a lineal response, samples of a same substance with different thickness will produce the same frequency spectrum. The linearity of the spectrometer can be affected, among other factors, by the response of the antennas and the signal amplification system.

To check the linearity we have chosen a method based in the measurements using a different number of silicon plates placed into the THz-beam path [22]. Even though silicon is quite transparent in the THz range, there is some radiation reflected at the plate polished faces which can be evaluated using the Fresnel coefficients. Every silicon plate will introduce the same losses, so measuring the peak maximum for a different number of interposed plates should produce a linear decrease of its amplitude.

We used 3 mm thick silicon plates separated the same distance of 3 mm. This plates are thicker than the etalon used for frequency calibration to avoid the formation of stationary waves as happens for the etalon measurements. In figure 3-a we show temporal pulses measured for an increasing number of plates interposed in the THz beam. There is an increasing delay of the maximum amplitude peak due to the optical path change introduced by the silicon plates

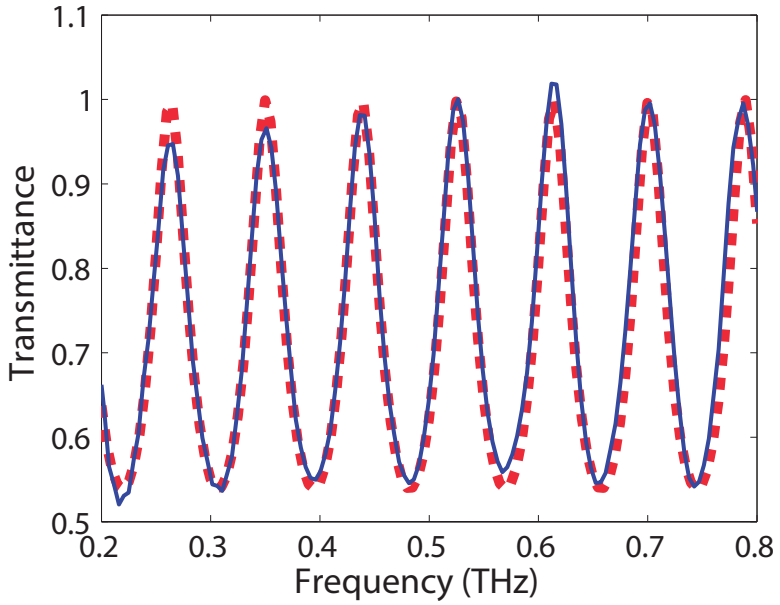

Figure 2: Transmittance measured by the spectrometer (continuous blue) and transmittance obtained with the Fabry-Perot model (dashed red).

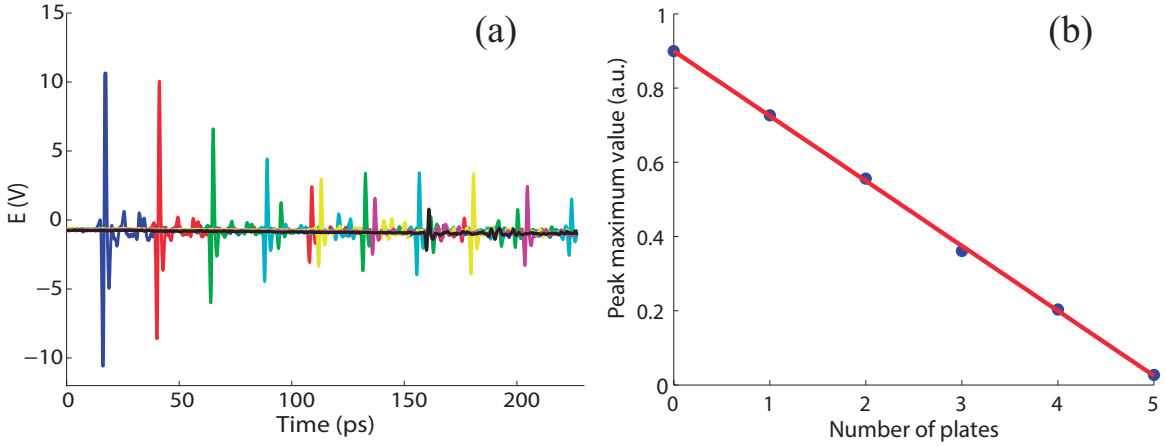

Figure 3: (a) Time domain measurements for different levels of attenuation of the THz radiation, obtained with the interposition of an increasing number of silicon plates. (b) Linear fit of the peak maximum value obtained for different number of silicon plates.

and also a progressive decrease of the peak amplitude due to the increasing reflection losses. In figure 3-b we plot the maximum amplitude value versus the number of plates. The points fit very well to a straight line revealing that the response is definitively linear.

3.3. Signal-to-noise ratio and dynamic range

Signal-to-noise ratio (SNR) and dynamic range (DR) are two parameters that determine the performance of the spectrometer. The SNR is defined as the ratio between the signal power and the noise power and measures the minimum signal change that it is possible to detect. On the

other hand the DR is the ratio from the maximum peak of the signal to the background noise and is a count of the maximum detectable signal change. Both parameters should be evaluated in both the spectral and time domains. These parameters are calculated, respectively, by using the expressions[23]:

$$SNR = \frac{\text{average value of the amplitude}}{\text{standard deviation of the amplitude}}, \quad (6)$$

$$DR = \frac{\text{maximum of the amplitude}}{\text{root mean square of noise}}. \quad (7)$$

To calculate the SNR and DR in both time and spectral domains, ten measurements in vacuum (no sample) are recorded and the spectral signal obtained with a fast Fourier transform (FFT). For each point of the time and spectral signal the average and standard deviation over the ten measurements are obtained. Also, a set of measurements were also done without THz signal in order to evaluate the root mean square of the background noise. This allows to calculate, using equations (6) and (7), both SNR and DR. For the SNR it was taken the value correspondent to the point of maximum signal amplitude. For the DR, it was taken the maximum value obtained all over the signal domain. Those values are given in table 1.

	SNR	DR (maximum)
Time domain	55	1100
Spectral domain	66	9066

Table 1: *Signal to noise ratio and dynamic range obtained for the spectrometer.*

3.4. Bandwidth and spectral resolution

The bandwidth and the spectral resolution are two parameters that determine the operating range of any spectrometer. Bandwidth is the frequency range in which most of the signal power is concentrated and the spectral resolution determines the minimum frequency shift that can be detected by the spectrometer. This parameters, respectively, are calculated by using the equations [5]:

$$\Delta\Omega = \frac{2\pi}{\delta t}, \quad (8)$$

$$\delta\omega = \frac{2\pi}{t_{sg}}, \quad (9)$$

where $\Delta\Omega$ is the bandwidth, δt is the sampling interval of the measured signal, $\delta\omega$ is the spectral resolution and t_{sg} is the duration of the measured temporal signal. For a typical measurement we acquired 1700 samples equally distributed in a scanning length of 3.4 cm (the maximum possible for motorized stage we employed). In this way, we have $\delta t = 1.3 \times 10^{-13}$ s and $t_{sg} = 2.3 \times 10^{-10}$ s and we consequently obtain $\Delta\Omega = 47$ THz and $\delta\omega = 0.027$ THz. These values are ideal but useful for a coarse estimation of the system performance. Other (non considered) factors have also influence on this parameters, limiting the performance of the system. Some of these factors are the stability and straightness of the stage, the laser beam quality, the efficiency of emitter and receiver antennas or the laser pulse duration.

3.5. Electric field
The electric field generated by the terahertz radiation can be calculated from the equation [5]

$$\overline{J} = \overline{N} e \mu E_{THz} \tag{10}$$

where $\overline{J}$ is the density of current, e is the electron charge, μ is the mobility of the charge carriers, $\overline{N}$ is the average number of charge carriers and E_{THz} is the THz electric field. For the calculation we take $\overline{N} = 2.5 \times 10^{22}\,\mathrm{m}^{-3}$, $\mu = 3000\,\mathrm{cm}^{-2}\,\mathrm{Vs}$ and $e = 1.602 \times 10^{-19}\,\mathrm{C}$ [24]. The amplification factor for the transimpedance amplifier is $10^5\,\mathrm{V/A}$ and the gain factor used in the lock-in amplifier is 3×10^3. The value of the photocurrent induced by the THz beam in the receiving antenna after passing through the plano-convex lens system is $I_{ph} = 33.3\,\mathrm{nA}$ for a focused laser beam of radius $r = 38\,\mu\mathrm{m}$. So, we get a value $E_{THz} = 0.6\,\mathrm{V/cm}$ for the electric field.

4. Application example
As an example of application of the reflection spectrometer, we present measurements intended to detect and evaluate the bandgap of a photonic crystal of the woodpile type. This type of 3D periodic structure consists of a number of layers each one formed by a set of long elements (cylinders) located parallel to each other in the plane. Consecutive layers are disposed with the elements relatively perpendicular, i. e. both planes are rotated 90 degrees, and cylinders belonging to every second plane present a relative shift of half a period [25]. This structure presents a tetragonal symmetry and if properly designed can be made to present a diamond-like face centered cubic (FCC) structure which corresponds to the case when the bandgap is the widest. For the existence of the bandgap, however, it is necessary a minimum value for the refractive index of the material.

Woodpile samples were fabricated of alumina (Al_2O_3), a highly transparent material at THz frequencies and presenting a dielectric constant of $\epsilon = 9.8$, using the direct ink writing (DIW) technique [26]. They present network constants of $d = 368\,\mu\mathrm{m}$ (separation between elements in plane) and $w = 153\,\mu\mathrm{m}$ (separation between planes of same-oriented cylinders). They were placed on the spectrometer and the THz beam focused on the face parallel to the piled planes. Spectrum measurements for incidence angles of zero (transmission), 45, 60 and 75 degrees (reflection) were recorded. Also, the same measurements were made on a homogeneous block sample for the sake of comparison. Results are plotted in figure 4.

The bandgap width depends on the tridimensional wavevector modulus and so the incidence angle of the radiation influences the values obtained. In the figure it is shown the presence of the bandgap centered on 0.3 THz approximately, where a deep valley in transmission is obtained respect to the block transmission. The bandgap is also detected by reflection as a hump in the reflectance curves. Maximum values of reflectance reach only values around 0.1 due to the high power loss as the samples measured where quite small and offered a small reflecting section to the THz beam.

5. Conclusion
In this work we have described a set up for TDS-THz spectroscopy by reflection. Details about the system and characteristics derived from its evaluation are presented. Finally, as an application example it was demonstrated its usefulness for the detection and measurement of the bandgap of a woodpile photonic crystal.

Acknowledgments
IFO acknowledges financial support from Xunta de Galicia, Spain (project EM2013/002).

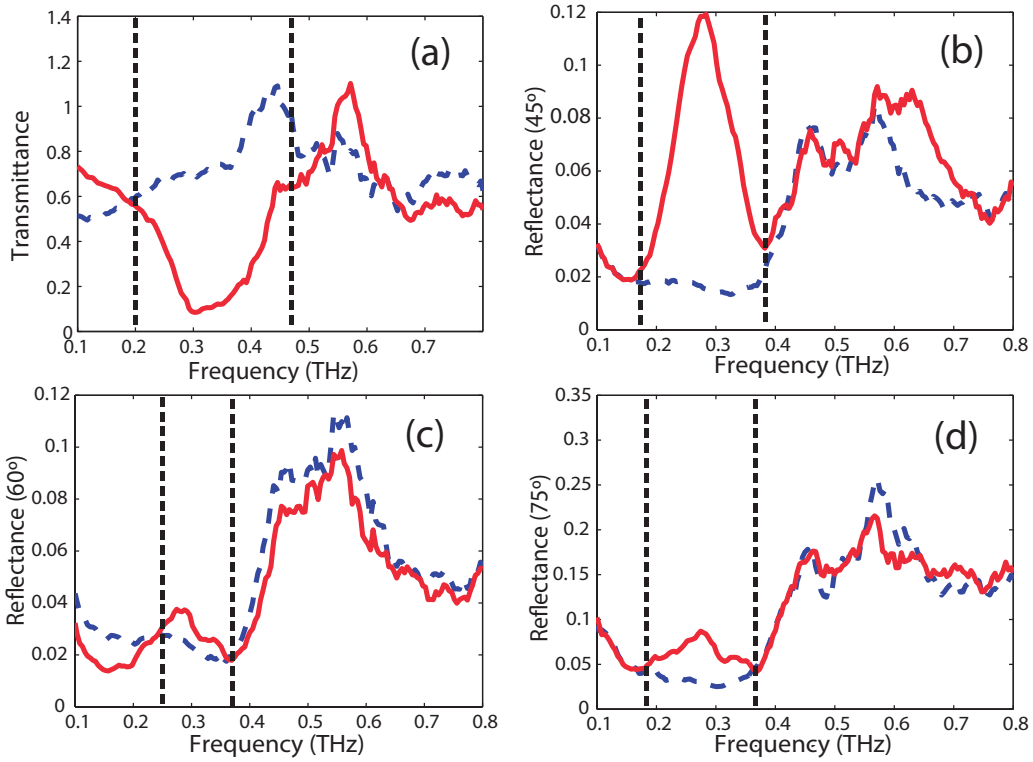

Figure 4: Measurements for a periodic structure sample of the woodpile type (continuous red line) as well as for an homogeneous block (dashed blue), both made of Al_2O_3. (a) Transmission (0 deg), (b) reflection at 45 deg, (c) reflection at 60 deg, (d) reflection at 75 deg. Vertical lines mark the bandgap region.

References

[1] Siegel P H 2002 *IEEE Trans. Microwave Theory Tech.* **50** 910–928

[2] Ferguson B and Zhang X C 2002 *Nature Mater.* **1** 26–33

[3] Tonouchi M 2007 *Nature Photon.* **1** 97–105

[4] Mueller E 2003 *The industrial physicist* 27–29

[5] Zhang X C and Xu J 2010 *Introduction to THz Wave Photonics* (New York: Springer)

[6] Pickwell E and Wallace V P 2006 *J. Phys. D: Appl. Phys.* **39**(17) R301–R310

[7] Oh S J, Kang J, Maeng I, Suh J S, Huh Y M, Haam S and Son J H 2009 *Opt. Express* **17** 3469–3475

[8] He M, Azad A K, Ye S and Zhang W 2006 *Opt. Commun.* **259** 389–392

[9] Strachan C J, Rades T, Newnham D A, Gordon K C, Pepper M and Taday P F 2004 *Chem. Phys. Lett.* **390**(1) 20–24

[10] Kurmbholtz N and et al 2009 *Milimetre Wave and Terahertz Sensors and Technology II* (*Proc. SPIE* vol 7485) p 748504

[11] Dickinson J C, Goyette T M, Gatesman A J, Joseph C S, Root Z G, Giles R H, Waldman J and Nixon W E 2006 **6212**

[12] Yamamoto K, Yamaguchi M, Miyamaru F, Tani M, Hangyo M, Ikeda T, Matsushita A, Koide K, Tatsuno M and Minami Y 2004 *Jpn. J. Appl. Phys.* **43**(No. 3B) L414 – L414–L417

[13] Redo-Sánchez A, Salvatella G, Galceran R, Roldós E, García-Reguero J A, Castellari M and Tejada J 2011 *Analyst* **136** 1733–1738

[14] Mittleman D, Jacobsen R, Neelamani R, Baraniuk R and Nuss M 1998 *Appl. Phys. B* **67** 379–390

[15] Dexheimer S L (ed) 2008 *Terahertz Spectroscopy: Principles and Applications* (Boca Raton: CRC Press)

[16] K E Peiponen Axel J and M K (eds) 2013 *Terahertz spectroscopy and imaging* first edition ed (New York: Springer)

[17] Lewis R A 2012 *Terahertz Physics* 1st ed (New York: Cambridge University Press)

[18] Matsuoka T, Fujimoto T, Tanaka K, Miyasaka S, Tajima S, Fujii K, Suzuki M and Tonouchi M 2009 *Physica C: Superconductivity* **469** 982–984

[19] Palka N 2011 *Acta Phys. Pol. A* **120** 713–715

[20] Pashkin A, Kempa M, Nemec H, Kadlec F and Kuzel P 2003 *Rev. Sci. Instrum.* **74** 4711–4717

[21] Naftaly M, Dudley R and Fletcher J 2010 *Opt. Commun.* **283** 1849 – 1853

[22] Naftaly M and Dudley R 2009 *Opt. Lett.* **34** 674–676

[23] Naftaly M and Dudley R 2009 *Opt. Lett.* **34**(8) 1213–1215

[24] Beard M C, Turner G M and Schmuttenmaer C A 2001 *J. Appl. Phys.* **90** 5915–5923

[25] Joannopoulos J D, Johnson S G, Winn J N and Meade R D 2008 *Photonic Crystals: Molding the Flow of Light* 2nd ed (Princeton, New Jersey: Princeton University Press)

[26] Smay J, Gratson G, Shepherd R, Cesarano J and Lewis J 2002 *Adv. Mater.* **14** 1279–1283